Plant Physiol. (1980) 66, 859-863
0032-0889/80/66/0859/05/$00.50/0

Growth-sustaining Water Potential Distributions in the Primary Corn Root

A NONCOMPARTMENTED CONTINUUM MODEL[1]

Received for publication September 18, 1979 and in revised form May 27, 1980

WENDY KUHN SILK AND KIT K. WAGNER
Department of Land, Air, and Water Resources, University of California, Davis, California 95616

ABSTRACT

An equation is derived from transport theory to relate local growth rate to local water potential in an expanding tissue. For a noncompartmented continuum model, the relative elemental growth rate (L) equals the divergence of the tensor product of hydraulic conductivity ($\underset{\sim}{K}$) and the gradient of water potential, Ψ, *i.e.* $L = \nabla\cdot[\underset{\sim}{K}\cdot\nabla\Psi]$. This equation is solved numerically using published values of L and $\underset{\sim}{K}$ to show the water potential distribution which can sustain the observed growth pattern in the primary root of *Zea mays* L. The water potential required to sustain growth decreases from the outside to the inside of the root, and the longitudinal profile shows most negative values near the location of the highest growth rate. A cell originally located near the apex experiences a loss and then a gain in water potential as it is displaced through the growth zone.

The approach differs from previous formulations in two respects: the assumption of spatial heterogeneity in growth rate, and the solution for spatial (site-specific) rather than material (cell-specific) values of water potential. The role of air spaces and of components (wall and possibly cytoplasm) of the water-conducting pathway which do not accumulate water remains to be clarified; and, as in earlier work, the most uncertain aspects of the analysis are probably the values for hydraulic conductivity.

Much of the large literature on plant water transport concerns flow through nongrowing tissues and deals with the often large Ψ[2] gradients in the soil-plant-atmosphere continuum. Recently, Molz and Boyer (13) made a pioneering study of Ψ distributions which would characterize a growing tissue. They showed that Ψ would become more negative along a line extending from a xylem element into the cortex of an elongating soybean hypocotyl. Below, an inhomogeneous distribution of growth rates is considered and a two-dimensional pattern of Ψ which can sustain growth of a corn root is found.

[1] This research was supported by National Science Foundation Grant PCM 78-23710.

[2] Abbreviations: Ψ, water potential; A, area of plant element in plane perpendicular to flux; $\underset{\sim}{g}$, growth velocity vector; $\underset{\sim}{J}$, water flux vector; $\underset{\sim}{K}$, hydraulic conductivity tensor; L, relative elemental growth rate (local strain rate); l, cell length; Q, volumetric flow rate; S, surface area of plant element; t, time; V, volume of plant element; x, distance; r, radial distance from root center line; z, longitudinal distance from root tip.

DERIVATION OF AN EQUATION RELATING LOCAL GROWTH RATE TO LOCAL Ψ

One can start with the approach of Philip (15) and discuss a cell which is expanding only in the direction of its long axis and which is in contact with water at only one end. For this one-dimensional system (Fig. 1, left) to a first approximation, the rate of volume increase (dV/dt) equals the rate of volumetric water flow (Q) into the cell. Furthermore, Q is proportional to the water flux, and, equivalently, to the growth velocity.

$$\frac{dV}{dt} = Q = AJ = Ag \tag{1}$$

where A is the cross-sectional area of the cell face perpendicular to the flow, g is the cell extension rate (growth velocity), and J is the water flux (volumetric flow rate/unit cross-sectional area).

Now, diverging from the earlier theory, a cell embedded in a continuum of expanding cells is considered (Fig. 1, right). For this cell, only water which is moving faster than wall 1 will cross the wall and enter the cell. In this case, the amount of water which flows into the cell equals the area of wall 1 times the velocity by which the water flux exceeds the rate of movement of the wall:

$$\text{Flow into the cell} = Q_1 = A(J_1 - g_1) \tag{2}$$

where g_1 is the growth velocity at 1; similarly

$$\text{Flow out of the cell} = Q_2 = A(J_2 - g_2) \tag{3}$$

where J_2 is the water flux at 2 and g_2 is the growth velocity at 2.

Since water is highly incompressible, its velocity does not change along the one-dimensional continuum. Therefore $J_1 = J_2$. The net flow of water into the expanding cell is equal to the difference between the inflow and the outflow so that the net flow (ΔQ) into the cell equals the cross-sectional area times the difference in growth rates between the apical and basal end of the cell:

$$\Delta Q = A(g_2 - g_1). \tag{4}$$

As in the simpler example above, the rate of volume change (dV/dt) in the deformable cell is equal to the net volumetric water flow into the cell:

$$\frac{dV}{dt} = \Delta Q = A(g_2 - g_1). \tag{5}$$

In three dimensions, equation 5 becomes

$$\frac{dV}{dt} = \oint (\underset{\sim}{J} - \underset{\sim}{g})\cdot\underset{\sim}{n}\, dS \tag{5a}$$

where $\underset{\sim}{n}$ is the unit normal to the surface.

Equation 5a shows that the rate of volume change of the cell which is instantaneously occupying the fixed volume V at a

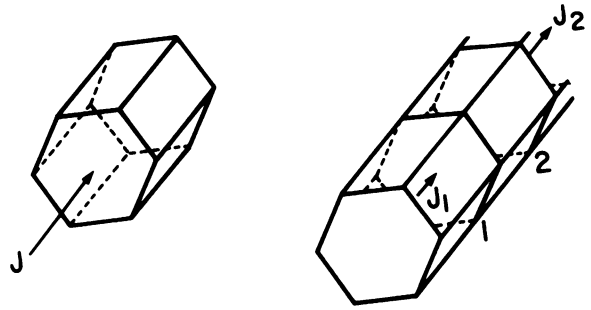

FIG. 1. Diagrams of water flux into plant cells: single cell (left) and cell embedded in a continuum of expanding cells (right).

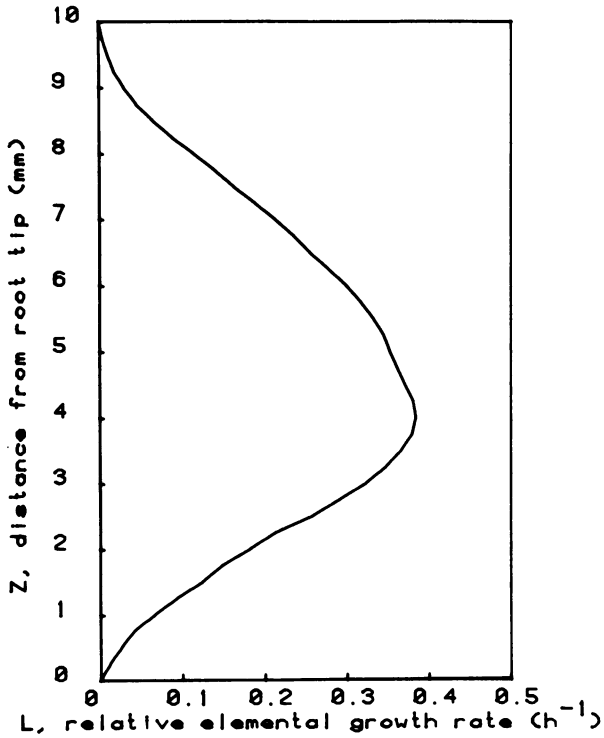

FIG. 2. Relative elemental growth rate or local strain rate (L) at different distances (Z) from the root tip (adapted from ref. 6).

particular location in space equals the sum (over the surface) of the components of $(\underline{J} - \underline{g})$ normal to the surface times the surface areas (dS) of the elements. Thus, growth velocity, as well as water velocity, enters into the expression for volumetric water flow into a cell. Next, the relationship between local growth rate and local Ψ is derived.

Water moves spontaneously from a region of high Ψ to a region of lower Ψ. Philip (16) reviewed a general model for water transport based on the Ψ gradient, and Molz (12, 14) developed the theory to include consideration of symplastic and apoplastic pathways. To summarize these models, in one dimension,

$$J = -K\frac{\partial \Psi}{\partial x} \tag{6}$$

where K, the hydraulic conductivity coefficient, and $\partial\Psi/\partial x$, the gradient of Ψ, are measurable at points, *i.e.* spatial locations.

In three dimensions, equation 6 becomes

$$\underline{J} = -\underline{\underline{K}} \cdot \nabla\Psi \tag{6a}$$

Equation 6a is the most general form of the laminar transport law for water moving in a noncompartmented medium. A field of scalar Ψ values exists in the medium, and $\nabla\Psi$, the gradient of this field at a point in the medium, is a vector in the direction of, and having the magnitude of, the maximum rate of change of Ψ. $\underline{\underline{K}}$ is a tensor, *i.e.* at the same point it may have different values in different directions; thus, the medium may be anisotropic in its resistance to water flow. Water flux is, in this general formulation, a vector field with local direction and magnitude determined by the interaction of the local conductivity with the local Ψ gradient. If hydraulic conductivity happens to be isotropic (equal in all directions), then the flux vector will have the same direction as the Ψ gradient; if $\underline{\underline{K}}$ is anisotropic, the flux will be twisted relative to the Ψ gradient.

To apply the Ψ equation 6 or 6a to a growing tissue, one must study a deformable element of the plant continuum (Fig. 1, right). This element occupies a given volume at a given time, and it must be noted once more that only water moving faster than the element boundary wall at 1 will enter the element. Therefore, to show the Ψ gradient which will cause water flux into the element (and, hence, element expansion), equation 6 must be modified:

$$(J - g) = -K\left(\frac{\partial \Psi}{\partial x}\right). \tag{7}$$

The net flow into the element is the difference between the inflow and outflow as formalized in equations 5 and 7. Proceeding as for equation 5, it is seen that

$$\frac{\Delta Q}{A} = (J_1 - g_1) - (J_2 - g_2) = -K_1\left(\frac{\partial \Psi}{\partial x}\right)_1 + K_2\left(\frac{\partial \Psi}{\partial x}\right)_2. \tag{8}$$

The disadvantage of this local measure of water flow is that its value depends on the length of the tissue segment we have chosen to study. One can circumvent the dependence on segment length by choosing very small segments and dividing by the length of the segment:

$$\lim_{\Delta x \to 0}\left[\frac{1}{\Delta x}((J_1 - g_1) - (J_2 - g_2))\right] = \lim_{\Delta x \to 0}\left[\frac{1}{\Delta x}\left(-K_1\left(\frac{\partial \Psi}{\partial x}\right)_1 + K_2\left(\frac{\partial \Psi}{\partial x}\right)_2\right)\right]. \tag{9}$$

Again, $(J_1 - J_2)$ is zero because water is incompressible; and equation 9 can be stated as

$$\frac{\partial g}{\partial x} = \frac{\partial}{\partial x} K\left(\frac{\partial \Psi}{\partial x}\right). \tag{10}$$

The velocity gradient on the left-hand side is recognizable as the relative elemental growth rate (5, 18) in one dimension, and the right-hand side is the spatial derivative of the product of $\underline{\underline{K}}$ and Ψ gradient. Generalizing to three dimensions, it can be seen that the fundamental relationship between growth and Ψ in a noncompartmented continuum model is given by

$$L = \nabla \cdot [\underline{\underline{K}} \cdot \nabla\Psi] \tag{10a}$$

i.e. the relative elemental growth rate (L) equals the divergence of the tensor product of $\underline{\underline{K}}$ and Ψ gradient. Compared to other formulations, equation 10a has the advantage that it relates growth at a point to Ψ at a point. The implication is that if the spatial distributions of L and $\underline{\underline{K}}$ are known, the growth-sustaining distributions of Ψ can, in theory, be calculated.

In practice, equation 10a is often difficult to solve. A special case which is suitable for many growing plant structures will be discussed. The following simplifying assumptions can often be made. (*a*) The tissue is cylindrical, with radius r, and growing only

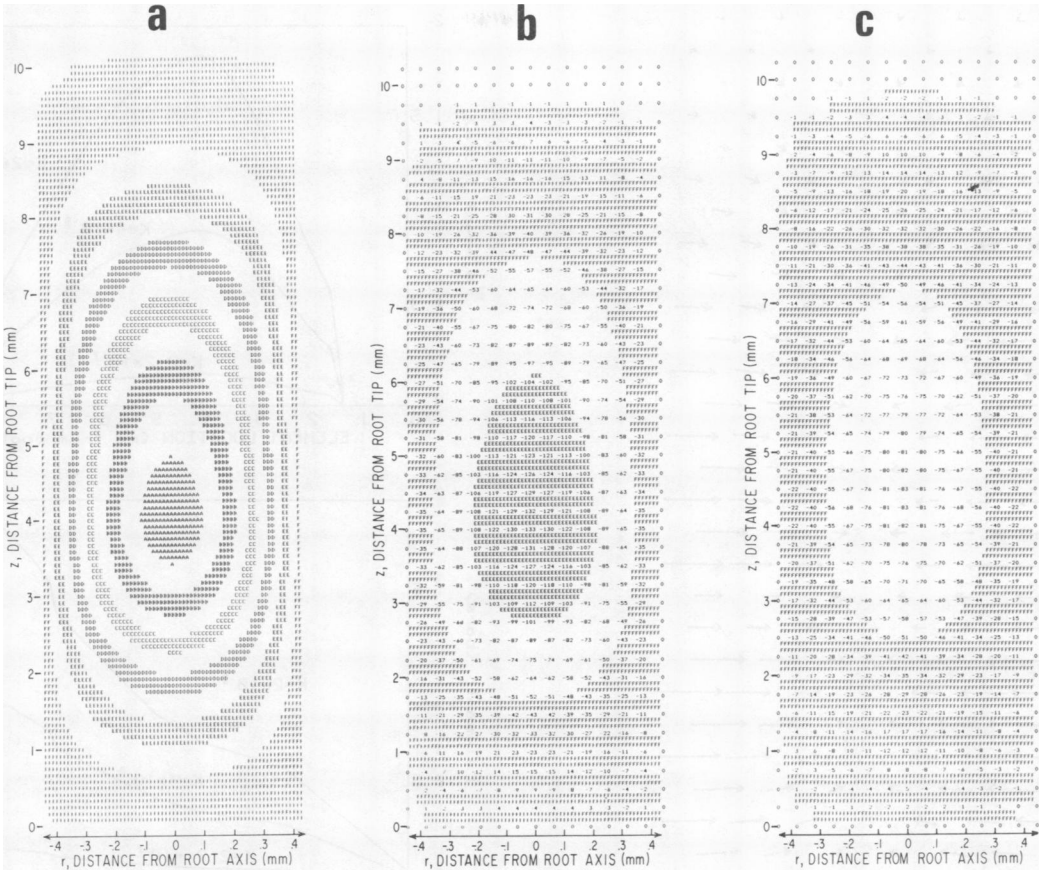

FIG. 3. Growth sustaining Ψ distributions in the primary corn root. Widths of the figures correspond to the diameter of the root median longisection; lengths are the length of the longisection extending through the growth zone. (Note difference in scale between z and r coordinates.) a, solution of equation 11 in terms of $K\Psi$, assuming K is isotropic and homogeneous. Letters represent regions of equal values of $K\Psi$ in $cm^2\ s^{-1}$: A, $-K\Psi > 5 \times 10^{-8}$; B, $4 \times 10^{-8} < -K\Psi < 4.5 \times 10^{-8}$; C, $3 \times 10^{-8} < -K\Psi < 3.5 \times 10^{-8}$; *D*, $2 \times 10^{-8} < -K\Psi < 2.5 \times 10^{-8}$; E, $10^{-8} < -K < 1.5 \times 10^{-8}$; and *F*, $-K\Psi < 5 \times 10^{-9}$. b, solution showing Ψ in centibars for a homogeneous $K = 4 \times 10^{-8}\ cm^2\ s^{-1}\ bar^{-1}$. c, solution showing Ψ in centibars when K_r ($cm^2\ s^{-1}\ bar^{-1}$) decreases from 8×10^{-8} at the tip to 4×10^{-8} at the base of the growth zone and $K_z = 8 \times 10^{-8}$ everywhere.

in the direction of its long axis. (*b*) The distribution of Ψ is axially symmetric. (*c*) The growth pattern does not change in time; therefore, the region of zero expansion moves in parallel with the growing tip; and the equation may be treated as a time independent problem with coordinate origin at the tip. It is recognized that the frame of reference is moving and that one is solving for spatial (site-specific) values of Ψ. (*d*) Conductivities in the radial (K_r) and longitudinal (K_z) directions are independent so that radial flow is not modified by longitudinal flow. If assumptions *a* to *d* are made, equation 10a becomes

$$K_z \frac{\partial^2 \Psi}{\partial z^2} + \frac{K_r}{r} \frac{\partial}{\partial r}\left(r \frac{\partial \Psi}{\partial r}\right) + \frac{\partial K_z}{\partial z}\frac{\partial \Psi}{\partial z} + \frac{\partial K_r}{\partial r}\frac{\partial \Psi}{\partial r} = L(z) \quad (11)$$

with $\partial\Psi/\partial t = 0$.

$L(z)$ can be determined experimentally (5, 18). If $\underset{\sim}{K}$ can be evaluated locally, then values of Ψ required to sustain the observed growth pattern can be computed.

SOLUTIONS OF LOCAL Ψ EQUATION 11

Equation 11 was solved with published values of L and $\underset{\sim}{K}$ in the primary corn root. The relative elemental growth rate distribution in the seedling root has been measured by Erickson and colleagues (4–6). The tabulated values of L (6) at 0.25-mm increments in the growth zone were used in the computations shown in Figure 3. It is helpful to keep in mind the shape of the *L versus* position curve (Fig. 2) in interpreting the Ψ distributions. The relative elemental growth rate (also termed the local stretch rate) has a maximum value of almost 0.40 h^{-1} at 4 mm from the root tip and falls to zero at 10 mm behind the root apex. To a first approximation, the plot of L against distance from the root tip is steady (independent of time) for more than 1 day, even though the cells located at a particular spot are continually displaced.

The literature also provides estimates of conductivity in the primary corn root (9). Ginsburg and Ginzburg (9) measured water flux across the root cortex in response to osmotic gradients introduced in the stele. They did not measure spatial variation in $\underset{\sim}{K}$ but provided a good base estimate of radial conductivity in the region just behind the growth zone. Using their data, and assuming that the Ψ gradient was constant across the cortex, we have calculated that $K_r = 4 \times 10^{-8}\ cm^2\ s^{-1}\ bar^{-1}$.

Equation 11, an elliptic partial differential equation, was solved numerically with an algorithm by Swartzrauber (19). The boundary conditions were to set $\Psi = 0$ at all boundaries. This means that the root was presumed to be growing without transpiring in pure water or completely saturated air. Thus, results are relative to zero Ψ in the bathing medium and the nongrowing region (Fig. 3). A general solution assuming isotropic homogeneous conductivities is given in Figure 3a, where each letter represents a narrow range of values of $K\Psi$, as indicated in the figure legend. The values are most negative in an egg-shaped region centered 4 mm from the tip in the middle of the cross-section. Comparison with Figure 2, which shows the local strain rate as a function of position, demonstrates that the most negative $K\Psi$ values coincide

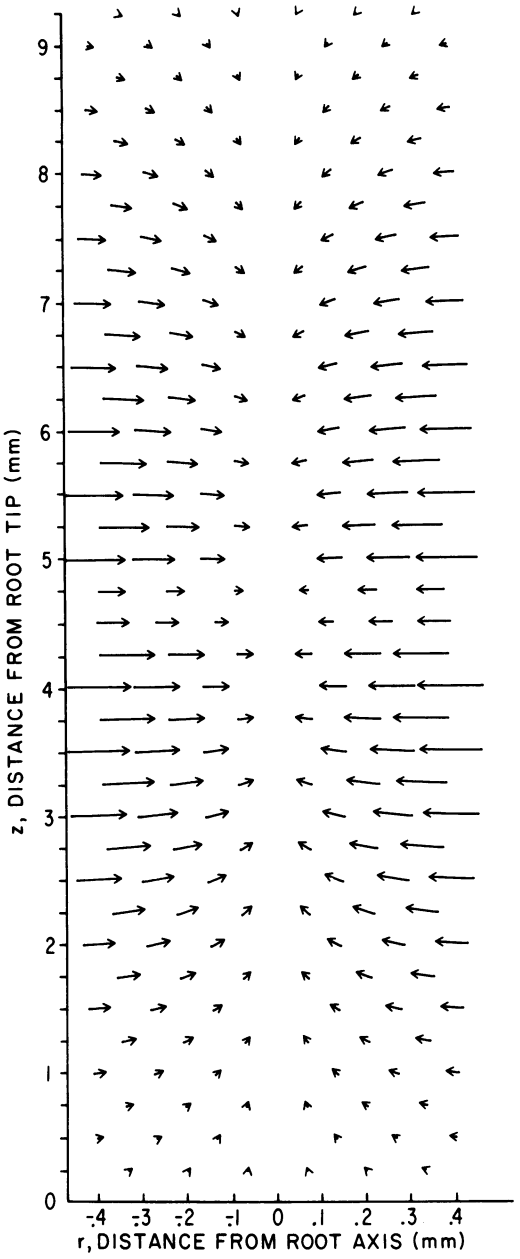

FIG. 4. Growth-sustaining water fluxes. Lengths of the arrows correspond to magnitudes of the local fluxes, and directions of arrows are in the local directions of flux calculated for conditions of Figure 3c.

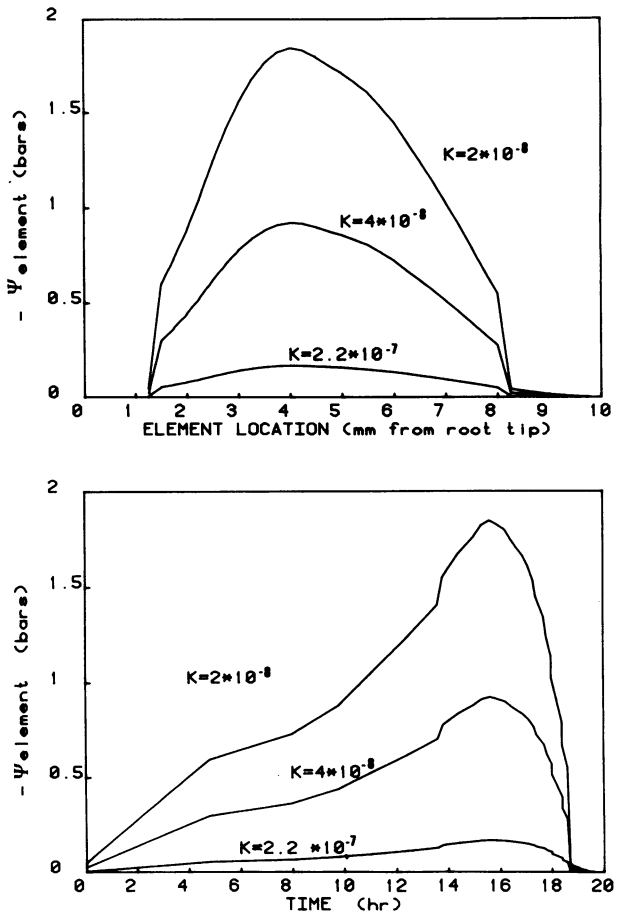

FIG. 5. Lagrangian (material or cell specific) specifications of Ψ for a root cortical cell as a function of position (upper graph) or time (lower graph). At time zero, the cell is located 1.2 mm behind the tip and 0.2 mm from the root surface. At later times, the cell experiences a more negative and then a less negative Ψ as it is displaced through the growth zone. Ψs are shown corresponding to spatially homogeneous $K = 10^{-8}$, $K = 2 \times 10^{-8}$, and $K = 10^{-7}$ cm^2 s^{-1} bar^{-1}.

with the region of largest strain rate. Concentric shells of progressively less negative values surround the central region. As a consequence of the assumption of axial symmetry, these shells are actually cross-sections of figures of revolution which exist in the three-dimensional structure; and it can be seen that the left-hand side of Figure 3a is the mirror image of the right-hand side. However, there is a decided asymmetry about the horizontal axis; the B, C, D, and E shells are thicker in the basal than the apical regions.

Estimates for growth-sustaining Ψ values given particular values of $\underset{\sim}{K}$ are shown in Figure 3, b and c. In both cases, Ψ decreases from the outside to the center of the root. And in both cases, the longitudinal distribution of Ψ shows that the point of most negative Ψ is close to the point of maximum growth rate. Figure 3b shows Ψ values for the same conditions (isotropic, homogeneous K) as in Figure 3a where $K = 4 \times 10^{-8}$ cm^2 s^{-1} bar^{-1}, as implied by the data of Ginsburg and Ginzburg (9). The most negative Ψ would be about -1.32 bars; and mean Ψ of a 1-mm thick circular disc in the region of most rapid growth would be 0.94 bars below the external Ψ.

On anatomical grounds, it seems likely that $\underset{\sim}{K}$ would vary with the direction of water movement in regions (distal to 4 mm) where the cells are not isodiametric. At 10 mm behind the tip, for instance, water moving in the radial direction would encounter fewer walls and membranes/unit cross-section than would water moving in the longitudinal direction. Study of the Molz model suggests that the anatomical anisotropy (if considered alone) would cause the root to be at most twice as conductive in the longitudinal as in the radial direction. The possible effect of anatomical anisotropy is tested in Figure 3c, where $K_r = K_z = 8 \times 10^{-8}$ cm^2 s^{-1} bar^{-1} at the root tip, and K_r decreases linearly with distance to 4×10^{-8} cm^2 s^{-1} bar^{-1} in the nongrowing zone. The computer solution is considerably more difficult in this case, but in Figure 3, comparison of b and c shows that the effect of the anisotropy is not very great in this range. The effect of spatial variation of K_r with r has not been tested here.

Figure 4 shows the distribution of water flux vectors in the growing zone. The arrows point in the direction of flux, and their lengths are proportional to the magnitude of the local flux. At any given distance from the tip, the flux is greatest at the root surface and decreases toward the interior. Flux magnitude at a given

distance from the root center parallels the local strain rate. The flux direction is predominantly radial at the surface of the root cylinder and throughout the root cross-section in the region of most rapid growth but, toward the ends of the growth zone, the interior fluxes are more nearly longitudinal. Near the longitudinal root axis, water moves vertically upward near the tip and vertically downward near the base of the growing region.

Figure 3 gives the static picture of Ψ at specific distances from the root tip. Any material (*i.e.* real) element of root, such as a cell, experiences changes in Ψ as it is displaced from the root tip. Figure 5 gives the material or Lagrangian specifications (17, 18) of Ψ for an element initially located 1.2 mm from the tip and 0.2 mm from the cylindrical surface. Steady growth is assumed, and displacement trajectories are calculated from Figure 8 of Erickson and Sax (6). The element experiences a decrease and then an increase in Ψ as it is displaced through the growth zone. These changes are shown for three possible values of $\underset{\approx}{K}$ within the suggested range (2). The element has its most negative Ψ at the location of fastest growth rate, 4 mm behind the tip, as shown in Figure 5. The time course for the material element is shown in the lower curves. It takes 16 h to acquire the most negative Ψ and only 3 h to reach negligible Ψ again. This is because the element accelerates from the tip to a constant displacement velocity at the base of the growth zone.

PHYSICAL SIGNIFICANCE OF SOLUTIONS SHOWN IN FIGURE 3

Ψ decreases from the outside to the center of the root. This is opposite in direction to the gradient shown by Molz and Boyer (13) because the water source bounds the root tissue externally rather than being supplied internally from the xylem as in the soybean hypocotyl. The same principle operates in both the stem and root example: to cause symplastic growth, Ψ must decrease with distance from the water supply. A water accumulation rate must be maintained which is constant throughout the element of cylinder cross-section. Furthermore, the water accumulation rate parallels the local stretch rate; hence, $K\Psi$ at a particular radial distance from the root center has its most negative value near the point of maximum relative elemental growth rate.

Equation 10a is a continuum version of the familiar equation which has been used in models of cell growth. Relative to Lockhart's (11) basic model for cell elongation, equation 10a can be viewed as a generalization to tissues of Lockhart's equation for the single cell

$$\frac{1}{l}\frac{dl}{dt} = K(\Delta\Psi)$$

where l is cell length, t is time, and K is shown as a product of permeability and geometry terms. The effects of local pressures and extensibilities in the continuum of expanding cells which make up the tissue could be studied in conjunction with equation 10a to obtain a general model for dynamics of tissue expansion.

Our estimates of K were derived from data of Ginsburg and Ginzburg (9); these estimates lie in the middle of the range which has been suggested (2) for growing tissue.

The most uncertain aspects of the analysis are these values for $\underset{\approx}{K}$s. There is no *a priori* theoretical reason to assume that $\underset{\approx}{K}$ is spatially homogeneous in a tissue characterized by a spatial gradient in developmental age. In fact, Boyer and Wu (1) have shown that auxin stimulation of growth in soybean hypocotyls is caused at least in part by an increase in $\underset{\approx}{K}$. The recent development of sensitive experimental methods to measure local conductivities offers hope of resolving the spatial variation in $\underset{\approx}{K}$ (7, 10). To solve equation 10a precisely, one must know this spatial pattern in the same growing tissue for which is known the distribution of the local strain rate.

Equation 10 and the solutions for the corn root should be considered phenomonological rather than mechanistic in nature. Cell structure is neglected, and K is a general tissue coefficient as opposed to σL_p, the membrane hydraulic conductivity of the more precise treatments from irreversible thermodynamics (2, 3, 8). Nevertheless, the utility of this approach is suggested by the demonstration (12, 14) that coupled flows in apoplasm and symplasm pathways can result in water movement which obeys the simple transport law. Local equilibrium between walls and cytoplasm is possible for many values of permeability, and Molz (12) has also shown that the diffusivity coefficient in the more complete and more complex model is numerically not too different from the diffusivity which would have been computed on Philip's (15) assumption of a noncompartmented cylinder. Thus, the treatment of the corn root as a noncompartmented system reported here can be expected to lead to reasonable predictions for growth-sustaining Ψ distributions.

Acknowledgments—The authors enjoyed an illuminating correspondence with F. Molz and J. Boyer and thank S. Whitaker and T. Hsiao for helpful conversations.

LITERATURE CITED

1. Boyer, JS, G Wu 1978 Water increases the hydraulic conductivity of auxin-sensitive hypocotyl tissue. Planta 139: 227–237
2. Dainty J 1963 Water relations of plant cells. Adv Bot Res 1: 279–326
3. Dainty J 1976 Water relations of plant cells. *In* U Luttge, Y Pittman, eds, Encyclopedia of Plant Physiology New Series, Vol. 2 Part A. Springer-Verlag, New York, pp 12–35
4. Erickson RO 1976 Modeling of plant growth. Annu Rev Plant Physiol 27: 407–434
5. Erickson RO, DR Goddard 1951 An analysis of root growth in cellular and biochemical terms. Growth Symp 10: 89–116
6. Erickson RO, KB Sax 1956 Elemental growth rate of the primary root of *Zea mays*. Proc Am Philos Soc 100: 487–498
7. Ferrier JM, J Dainty 1977 A new method for measurement of hydraulic conductivity and elastic coefficients in higher plant cells using an external force. Can J Bot 55: 858–866
8. Fiscus EL, PJ Kramer 1975 General model for osmotic and pressure-induced flow in plant roots. Proc Natl Acad Sci USA 72: 3114–3118
9. Ginsburg H, BZ Ginzburg 1970 Radial water and solute flows in roots of *Zea mays*. J Exp Bot 21: 580–592
10. Hüsken D, E Steudle, U Zimmermann 1978 Pressure probe technique for measuring water relations of cells in higher plants. Plant Physiol 61: 158–163
11. Lockhart J 1965 Cell extension. *In* A Bonner, B Varner, eds, Plant Biochemistry. Academic Press, New York, pp 826–849
12. Molz FJ 1976 Water transport through plant tissue: the apoplasm and symplasm pathways. J Theor Biol 9: 277–292
13. Molz FJ, JS Boyer 1978 Growth-induced water potentials in plant cells and tissues. Plant Physiol 62: 423–429
14. Molz FJ, E Ikenberry 1974 Water transport through plant cells and cell walls: theoretical development. Soil Sci Soc Am J 38: 699–704
15. Philip JR 1958 Propagation of turgor and other properties through cell aggregations. Plant Physiol 33: 271–274
16. Philip JR 1966 Plant water relations: some physical aspects. Annu Rev Plant Physiol 17: 245–268
17. Silk MWK, RO Erickson 1978 Kinematics of hypocotyl curvature. Am J Bot 65: 310–319
18. Silk MWK, RO Erickson 1979 Kinematics of plant growth. J Theor Biol 76: 481–501
19. Swarztrauber PN 1974 A direct method for the discrete solution of separable elliptic equations. SIAM J Numer Anal 11: 1136–1150
20. Zimmermann U, E Steudle 1978 Physical aspects of water relations of plant cells. Adv Bot Res 6: 46–112